



**Table 1**

Selected geometric parameters (Å, °) for **1**.

Au1–N11	2.070 (3)	Au1–Cl2	2.2832 (10)
Au1–Cl3	2.2826 (10)	Au1–Cl1	2.3006 (10)
N11–Au1–Cl3	93.13 (11)	Cl2–Au1–Cl1	91.18 (4)
N11–Au1–Cl2	85.80 (11)	Cl6–N11–Cl2	110.6 (3)
Cl3–Au1–Cl2	178.07 (4)	Cl6–N11–Au1	117.8 (3)
N11–Au1–Cl1	176.94 (11)	Cl2–N11–Au1	111.0 (3)
Cl3–Au1–Cl1	89.90 (4)		
Cl3–Au1–N11–Cl6	–30.0 (3)	Au1–N11–Cl2–Cl3	169.1 (3)
Cl2–Au1–N11–Cl6	151.6 (3)	Cl2–Cl3–Cl4–Cl7	179.8 (4)
Cl3–Au1–N11–Cl2	98.8 (3)	C17–Cl4–Cl5–Cl6	179.4 (4)
Cl2–Au1–N11–Cl2	–79.6 (3)	Au1–N11–Cl6–Cl5	–172.6 (3)

**Table 2**

Selected geometric parameters (Å, °) for **2a**.

Au1–N11	2.096 (5)	Au1–Br3	2.4110 (7)
Au1–Br1	2.4066 (7)	Au1–Br2	2.4273 (6)
N11–Au1–Br1	179.50 (15)	Br1–Au1–Br2	91.68 (2)
N11–Au1–Br3	91.78 (15)	Br3–Au1–Br2	179.60 (2)
Br1–Au1–Br3	88.72 (2)	C12 <sup>i</sup> –N11–Cl2	111.2 (5)
N11–Au1–Br2	87.82 (15)	C12 <sup>i</sup> –N11–Au1	113.4 (3)
Br3–Au1–N11–Cl2	–64.1 (3)	Au1–N11–Cl2–Cl3	–174.4 (3)
Br2–Au1–N11–Cl2	115.9 (3)	Cl2–Cl3–Cl4–Cl5	–179.7 (4)

Symmetry code: (i)  $x, -y + \frac{3}{2}, z$ .

**Table 3**

Selected geometric parameters (Å, °) for **2b**.

Au1–N11	2.094 (4)	Au1–Br2	2.4244 (5)
Au1–Br1	2.4187 (5)	Au1–Br3	2.4246 (5)
N11–Au1–Br1	176.50 (11)	Br2–Au1–Br3	177.736 (17)
N11–Au1–Br2	86.00 (11)	C12–N11–Cl6	110.9 (4)
Br1–Au1–Br2	90.665 (18)	C12–N11–Au1	111.6 (3)
N11–Au1–Br3	93.62 (11)	C16–N11–Au1	117.8 (3)
Br1–Au1–Br3	89.751 (18)		
Br2–Au1–N11–Cl2	–78.0 (3)	Au1–N11–Cl2–Cl3	168.1 (3)
Br3–Au1–N11–Cl2	99.8 (3)	Cl2–Cl3–Cl4–Cl7	–179.2 (4)
Br2–Au1–N11–Cl6	152.0 (3)	C17–Cl4–Cl5–Cl6	178.9 (4)
Br3–Au1–N11–Cl6	–30.2 (3)	Au1–N11–Cl6–Cl5	–171.6 (3)

carbon at C-4 and the methyl carbon (these atoms are numbered for **2a** as C14 and C15). For all three structures, the halogen atoms are numbered such that  $X1$  ( $X = \text{halogen}$ ) is

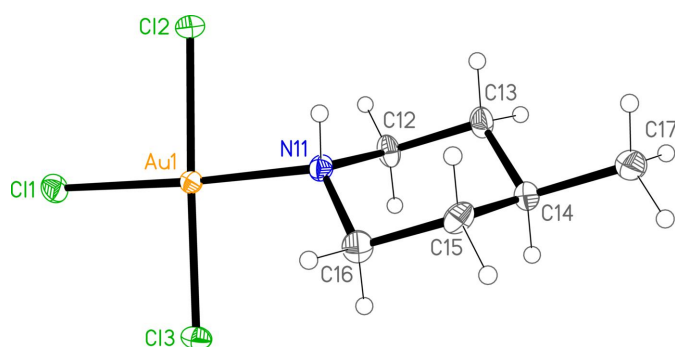


**Figure 1**

The structure of compound **1** in the crystal. Ellipsoids correspond to 50% probability levels.

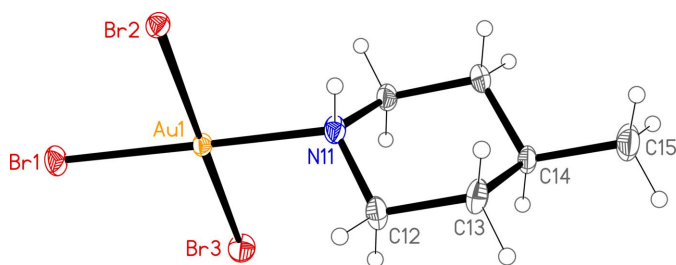


**Figure 2**

The structure of compound **2a** in the crystal. Ellipsoids correspond to 50% probability levels. Only the asymmetric unit is numbered.

*trans* to the ligand nitrogen atom N11. Structures **1** and **2b** are isotopic. The geometry at the gold atoms is as expected square planar. Bond lengths and angles (Tables 1–3) may be considered normal. The Au–N bonds *trans* to Cl are somewhat shorter than those *trans* to Br, and the Au–Cl bonds *trans* to N are longer than those *cis* to N, whereas the Au–Br bonds *trans* to N are slightly shorter than the *cis* bonds. Similar trends were observed for (pip)AuCl<sub>3</sub> and (pip)AuBr<sub>3</sub> (Döring & Jones, 2023a).

The relative orientation of the ligand and the AuX<sub>3</sub> unit is described by the torsion angles  $Xn\text{--}Au1\text{--}N11\text{--}H01$  and  $Xn\text{--}Au1\text{--}N11\text{--}C$ , where  $n = 2$  or 3 (torsion angles for  $n = 1$  are meaningless because the sequence  $X1\text{--}Au1\text{--}N1$  is linear). We observe two distinct types: either one angle  $Xn\text{--}Au1\text{--}N11\text{--}H01$  is approximately zero, corresponding to a short  $H01\cdots Xn$  contact that might be considered an intramolecular hydrogen bond, and the smallest absolute  $Xn\text{--}Au1\text{--}N11\text{--}C$  angle is around 60°, or the angle  $Xn\text{--}Au1\text{--}N11\text{--}H01$  is approximately 30–40° and the smallest absolute  $Xn\text{--}Au1\text{--}N11\text{--}C$  angle is around 30°. The former type applies to (pip)AuCl<sub>3</sub> and **2a** [where  $Br2\text{--}Au1\text{--}N11\text{--}H01$  is exactly zero by symmetry and  $H01\cdots Br2$  is 2.71 (6) Å], and the latter to (pip)AuBr<sub>3</sub>, **1** and **2b**.

As would be expected for bulky substituents attached to cyclohexane-type rings, the methyl groups and the AuX<sub>3</sub> moieties occupy equatorial positions, with torsion angles  $C\text{--}C\text{--}N\text{--}Au$  and  $C\text{--}C\text{--}C\text{--}C_{\text{methyl}}$  around  $\pm 180^\circ$ . Our previous two papers however include several structures where

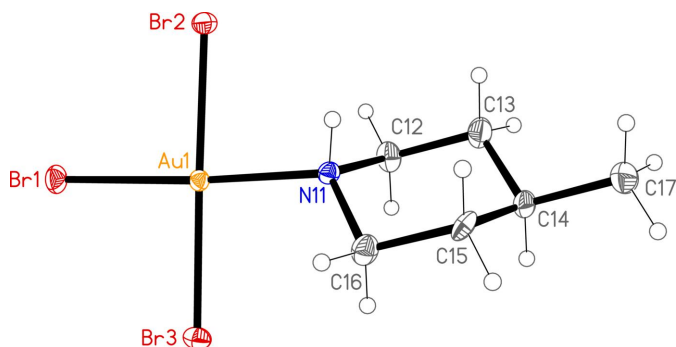


**Figure 3**

The structure of compound **2b** in the crystal. Ellipsoids correspond to 50% probability levels.

**Table 4**  
 Hydrogen-bond geometry (Å, °) for **1**.

<i>D</i> —H··· <i>A</i>	<i>D</i> —H	H··· <i>A</i>	<i>D</i> ··· <i>A</i>	<i>D</i> —H··· <i>A</i>
N11—H01···Cl1 <sup>i</sup>	0.93 (4)	2.64 (4)	3.535 (4)	163 (4)
C15—H15B···Cl1 <sup>i</sup>	0.99	2.97	3.804 (4)	143
C13—H13B···Cl2 <sup>ii</sup>	0.99	2.82	3.798 (4)	171
C15—H15A···Cl3 <sup>iii</sup>	0.99	2.95	3.610 (4)	125
C15—H15A···Cl3 <sup>iv</sup>	0.99	2.99	3.728 (4)	132
C16—H16B···Cl3 <sup>i</sup>	0.99	2.91	3.656 (5)	133

Symmetry codes: (i)  $-x + \frac{1}{2}, y + \frac{1}{2}, z$ ; (ii)  $x + \frac{1}{2}, -y + \frac{1}{2}, -z$ ; (iii)  $-x + 1, y + \frac{1}{2}, -z + \frac{1}{2}$ ; (iv)  $x + \frac{1}{2}, y, -z + \frac{1}{2}$ .

**Table 5**  
 Hydrogen-bond geometry (Å, °) for **2a**.

<i>D</i> —H··· <i>A</i>	<i>D</i> —H	H··· <i>A</i>	<i>D</i> ··· <i>A</i>	<i>D</i> —H··· <i>A</i>
N11—H01···Br2	0.89 (6)	2.71 (6)	3.146 (5)	111 (5)
C12—H12B···Br1 <sup>ii</sup>	0.99	2.94	3.786 (5)	145
C12—H12B···Br2 <sup>ii</sup>	0.99	2.99	3.798 (4)	139
C15—H15A···Br2 <sup>iii</sup>	0.97	2.98	3.936 (7)	169
C12—H12A···Br3	0.99	2.96	3.526 (4)	118
C13—H13A···Br3 <sup>iv</sup>	0.99	3.09	4.002 (4)	154
C15—H15B···Br3 <sup>iv</sup>	0.98	3.05	3.965 (3)	155

Symmetry codes: (ii)  $-x, -y + 2, -z$ ; (iii)  $x + \frac{1}{2}, y, -z - \frac{1}{2}$ ; (iv)  $-x + 1, -y + 2, -z$ .

**Table 6**  
 Hydrogen-bond geometry (Å, °) for **2b**.

<i>D</i> —H··· <i>A</i>	<i>D</i> —H	H··· <i>A</i>	<i>D</i> ··· <i>A</i>	<i>D</i> —H··· <i>A</i>
N11—H01···Br1 <sup>i</sup>	0.97 (4)	2.81 (4)	3.759 (4)	164 (4)
C12—H12A···Br2	0.99	2.99	3.542 (5)	116
C13—H13B···Br2 <sup>ii</sup>	0.99	2.93	3.903 (5)	169
C16—H16B···Br3 <sup>i</sup>	0.99	2.99	3.750 (5)	135

Symmetry codes: (i)  $-x + \frac{1}{2}, y + \frac{1}{2}, z$ ; (ii)  $x + \frac{1}{2}, -y + \frac{1}{2}, -z$ .

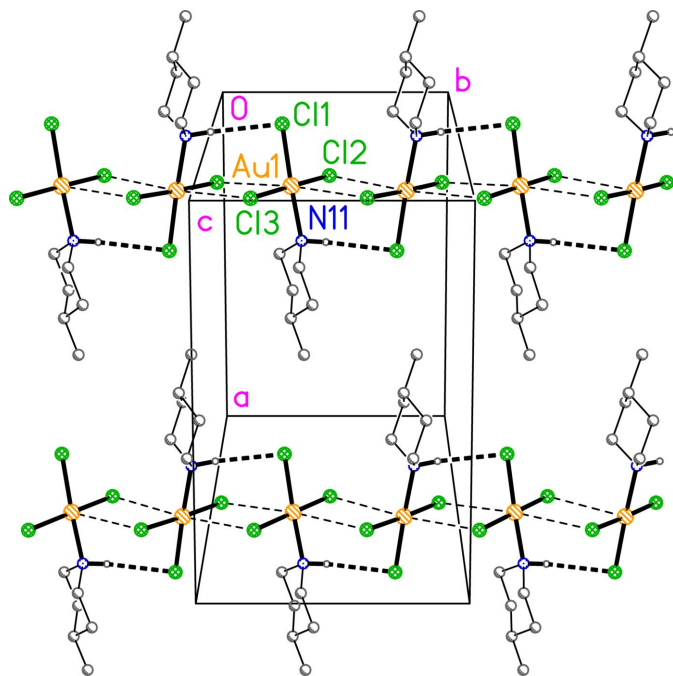


**Figure 4**  
 Packing diagram of compound **1** viewed approximately parallel to the *c* axis (but rotated by  $ca\ 15^\circ$  around the horizontal axis for clarity) in the region  $z \approx 0.125$ , showing two chains of molecules parallel to the *b* axis. Dashed lines indicate H···Cl hydrogen bonds (thick) or Au···Cl contacts (thin). Hydrogen atoms not involved in hydrogen bonding are omitted. Atom labels indicate the asymmetric unit. Similar chains are formed in the regions  $z \approx 0.375, 0.625$  and  $0.875$ .

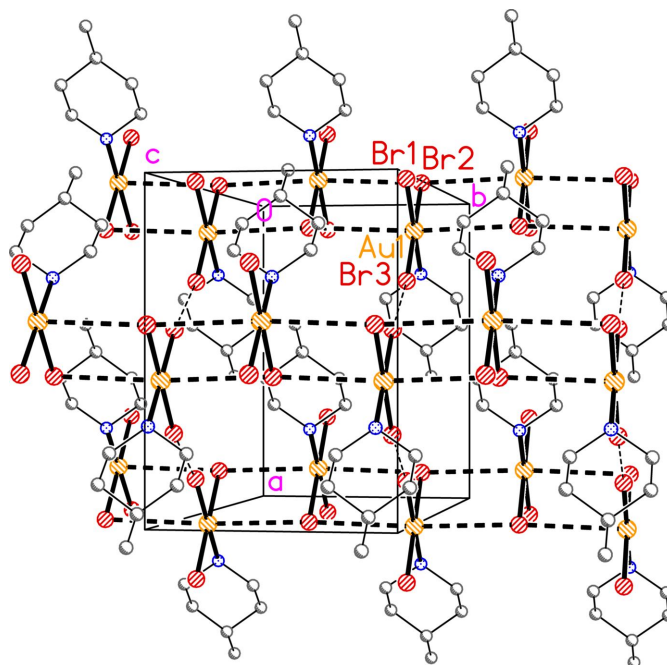


**Figure 5**  
 Packing diagram of compound **2a** viewed approximately parallel to the *c* axis (but rotated by  $ca\ 10^\circ$  about the vertical axis for clarity), showing three chains of molecules parallel to the *b* axis. The chains are centred on the regions  $(x, z) = (0, 0), (1, 0)$  and  $(1/2, 1/2)$ . Dashed lines indicated Au···Br contacts (thick) or Br···Br contacts (thin); the latter are shown more clearly in Fig. 6. Atom labels indicate the asymmetric unit.

a gold(I) atom occupies an axial position in similar molecules. The ‘normal’ equatorial positions observed for **1**, **2a** and **2b** may be associated with steric effects, which should be greater for the larger AuX<sub>3</sub> moieties compared to the linear gold(I) centres.

### 3. Supramolecular features

For compound **1**, the main intermolecular contacts are the hydrogen bond N1—H01···Cl1( $\frac{1}{2} - x, \frac{1}{2} + y, z$ , the *b* glide operator) and the two Au···Cl contacts Au1···Cl3 (same operator) = 3.2980 (10) Å and Au1···Cl2( $\frac{1}{2} - x, -\frac{1}{2} + y, z$ ) = 3.3604 (10) Å that correspond to an offset stacking of the AuCl<sub>3</sub> moieties. These combine to form chains of molecules parallel to the *b* axis (Fig. 4). In the isotopic **2b**, the corresponding Au···Br distances are 3.4060 (5) and 3.5018 (5) Å.

Compound **2a** forms chains analogous to those of **1**, with Au1···Br2( $-x, 1 - y, -z$  and  $-x, 2 - y, -z$ ) = 3.5847 (2) Å; these run parallel to the *b* axis (Fig. 5). The chains are cross-linked by short Br···Br contacts involving one *cis* (to N) and the *trans* Br atom, with Br1···Br3( $-\frac{1}{2} + x, y, \frac{1}{2} - z$ , the *a* glide operator) = 3.3686 (6) Å and angles Au1—Br1···Br3′ = 166.26 (3) and Au1—Br3···Br1′ = 162.77 (3)°. These contacts are indicated in Fig. 5 but are shown more clearly in Fig. 6; they link the molecules to form chains parallel to the *b* axis. The NH group is not involved in intermolecular hydrogen bonding.

All three structures also display C—H···X contacts that might be interpreted as ‘weak’ hydrogen bonds (Tables 4–6),

**Table 7**  
Experimental details.

	<b>1</b>	<b>2a</b>	<b>2b</b>
Crystal data			
Chemical formula	[AuCl <sub>3</sub> (C <sub>6</sub> H <sub>13</sub> N)]	[AuBr <sub>3</sub> (C <sub>6</sub> H <sub>13</sub> N)]	[AuBr <sub>3</sub> (C <sub>6</sub> H <sub>13</sub> N)]
<i>M<sub>r</sub></i>	402.49	535.87	535.87
Crystal system, space group	Orthorhombic, <i>Pbca</i>	Orthorhombic, <i>Pnma</i>	Orthorhombic, <i>Pbca</i>
Temperature (K)	100	100	100
<i>a</i> , <i>b</i> , <i>c</i> (Å)	12.5716 (6), 8.3940 (3), 20.3319 (7)	9.9871 (5), 7.1505 (4), 15.7160 (8)	12.6471 (5), 8.7247 (3), 21.0262 (7)
<i>V</i> (Å <sup>3</sup> )	2145.53 (14)	1122.32 (10)	2320.07 (15)
<i>Z</i>	8	4	8
Radiation type	Mo <i>K</i> α	Mo <i>K</i> α	Mo <i>K</i> α
μ (mm <sup>-1</sup> )	14.40	23.74	22.96
Crystal size (mm)	0.22 × 0.03 × 0.01	0.27 × 0.06 × 0.03	0.14 × 0.04 × 0.03
Data collection			
Diffractometer	Oxford Diffraction Xcalibur, Eos	Oxford Diffraction Xcalibur, Eos	Oxford Diffraction Xcalibur, Eos
Absorption correction	Multi-scan ( <i>CrysAlis PRO</i> ; Rigaku OD, 2015)	Multi-scan ( <i>CrysAlis PRO</i> ; Rigaku OD, 2015)	Multi-scan ( <i>CrysAlis PRO</i> ; Rigaku OD, 2015)
<i>T<sub>min</sub></i> , <i>T<sub>max</sub></i>	0.702, 1.000	0.240, 1.000	0.380, 1.000
No. of measured, independent and observed [ <i>I</i> > 2σ( <i>I</i> )] reflections	53277, 2887, 2134	28605, 1864, 1581	38297, 3371, 2495
<i>R<sub>int</sub></i>	0.080	0.070	0.074
θ values (°)	θ <sub>max</sub> = 29.1, θ <sub>min</sub> = 2.6	θ <sub>max</sub> = 31.1, θ <sub>min</sub> = 2.4	θ <sub>max</sub> = 30.0, θ <sub>min</sub> = 2.5
Refinement			
<i>R</i> [ <i>F</i> <sup>2</sup> > 2σ( <i>F</i> <sup>2</sup> )], <i>wR</i> ( <i>F</i> <sup>2</sup> ), <i>S</i>	0.024, 0.042, 1.05	0.030, 0.050, 1.11	0.029, 0.043, 1.04
No. of reflections	2887	1864	3371
No. of parameters	105	65	105
H-atom treatment	H atoms treated by a mixture of independent and constrained refinement	H atoms treated by a mixture of independent and constrained refinement	H atoms treated by a mixture of independent and constrained refinement
Δρ <sub>max</sub> , Δρ <sub>min</sub> (e Å <sup>-3</sup> )	0.86, -0.86	1.56, -1.19	0.99, -0.99

Computer programs: *CrysAlis PRO* (Rigaku OD, 2015), *SHELXS97* (Sheldrick, 2008), *SHELXL2019/3* (Sheldrick, 2015) and *XP*, (Bruker, 1998).

but none of these is strikingly short. These (and other) weak interactions might well contribute significantly to the packing energy, but it is difficult to incorporate them in easily interpretable packing diagrams.

#### 4. Database survey

The searches employed the routine ConQuest (Bruno *et al.*, 2002), part of Version 2023.3.0 of the Cambridge Database (Groom *et al.*, 2016). A search for short Cl⋯Cl contacts between molecules *LAuCl*<sub>3</sub> (*L* = any atom) gave 51 hits (59 independent molecules) with contact distances from 3.086 to 3.37 Å and an average Au—Cl⋯Cl angle of 152.9°. A similar search for *LAuBr*<sub>3</sub> (*L* = any atom) gave 28 hits (36 independent molecules) with contact distances from 3.26 to 3.67 Å and an average Au—Br⋯Br angle of 150.7°. The upper bounds for the contact distances in both cases correspond to the double van der Waals radii as stored in the CCDC. For both sets of results, the *cis* (to *L*) halogen atoms were more often involved than the *trans* halogen atoms (the latter corresponding to *X1* in the structures presented here); for *X* = Cl there were 9 contacts of the form *trans/trans*, 5 *cis/trans* and 37 *cis/cis*, and the corresponding values for *X* = Br were 4, 7 and 25. In many cases, the Au—*X*⋯*X* angles were equal by symmetry, and both values were used to calculate the average values.

#### 5. Synthesis and crystallization

The starting materials of choice would be the gold(I) complexes (4-Me-pip)Au*X*, but these exist in the ionic form [(4-Me-pip)<sub>2</sub>Au][Au*X*<sub>2</sub>] rather than as neutral molecules (Döring & Jones, 2024).

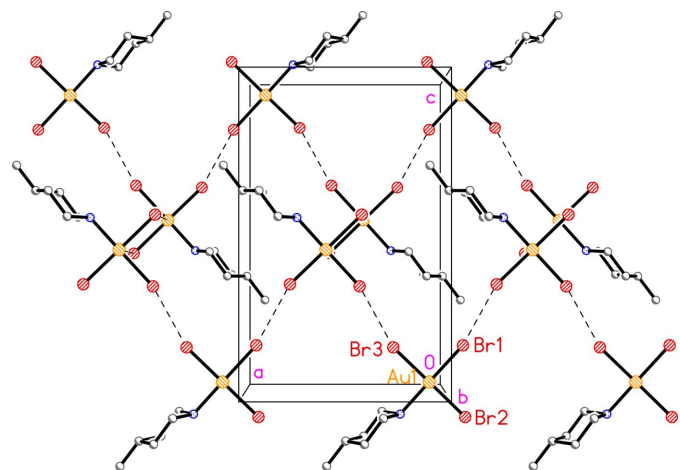


**Figure 6**  
Packing diagram of compound **2a** showing two zigzag chains of molecules parallel to the *b* axis; the lower chain is centred in the mirror plane at *y* = 0.75 and the upper chain in the plane at *y* = 0.25. Dashed lines indicated Br⋯Br contacts (or, just visible, Au⋯Br contacts linking the two chains in the direction into the paper). Atom labels indicate the asymmetric unit.



*Trichlorido(4-methylpiperidine)gold(III) (1)*

A solution of bis(4-methylpiperidine)gold(I) dichloridoaurate(I) (310 mg, 0.454 mmol) in 4 mL of dichloromethane was added to a solution of PhICl<sub>2</sub> (125 mg, 0.454 mmol) in 3 mL of dichloromethane. 2 mL of the mixed solution were divided amongst five small test-tubes and overlaid with various precipitants. The tubes were then stoppered and stored in a refrigerator at 276 K. The measured crystal was obtained using diisopropyl ether as precipitant. Elemental analysis [%]: calc. C 17.91, H 3.26, N 3.48; found C 17.64, H 3.30, N 3.65.

*Tribromido(4-methylpiperidine)gold(III) (2)*

Polymorph **2a**: Bis(4-methylpiperidinium) bromide tetrabromidoaurate(III), {(4-Me-pip)H}<sub>2</sub>·Br·[AuBr<sub>4</sub>] (Döring, 2016) (26 mg, 0.0327 mmol) was dissolved in 1.5 mL of dichloromethane. The solution was divided amongst three small test tubes and overlaid with various precipitants. The tubes were then stoppered and stored in a refrigerator at 276 K. Using diisopropyl ether as precipitant, a mixture of crystals of the starting material (structure to be reported elsewhere) and of **2a** was obtained.

Polymorph **2b**: Bis(4-methylpiperidine)gold(I) dibromidoaurate(I), [(4-Me-pip)<sub>2</sub>Au][AuBr<sub>2</sub>], (90 mg, 0.239 mmol) was dissolved in 2 mL of dichloromethane and two drops of elemental bromine were added. The solution was overlaid with diisopropyl ether and stored in a refrigerator at 276 K, whereby crystals of **2b** formed.

**6. Refinement**

Details of the measurements and refinements are given in Table 7. Structures were refined anisotropically on  $F^2$ . For all compounds, the NH hydrogen atoms were refined freely. Methylene hydrogens were included at calculated positions and refined using a riding model with C—H = 0.99 Å and

H—C—H = 109.5°. Methine hydrogens were included similarly, but with C—H = 0.99 Å. Methyl groups were included as idealized rigid groups with C—H 0.98 Å and H—C—H 109.5°, and were allowed to rotate but not to tip (command 'AFIX 137').  $U$  values of the hydrogen atoms were fixed at  $1.5 \times U_{\text{eq}}$  of the parent carbon atoms for methyl groups and  $1.2 \times U_{\text{eq}}$  of the parent carbon atoms for other hydrogens. For compound **2a**, an extinction correction was performed; the extinction parameter (Sheldrick, 2015) refined to 0.00051 (4).

**Acknowledgements**

We gratefully acknowledge support by the Open Access Publication Funds of the Technical University of Braunschweig.

**References**

- Bruker (1998). *XP*. Bruker Analytical X-Ray Instruments, Madison, Wisconsin, USA.
- Bruno, I. J., Cole, J. C., Edgington, P. R., Kessler, M., Macrae, C. F., McCabe, P., Pearson, J. & Taylor, R. (2002). *Acta Cryst.* **B58**, 389–397.
- Döring, C. (2016). *Halogen(I)-Aminkomplexe und ihre Oxidationsprodukte*. Dissertation, Technical University of Braunschweig, Germany. ISBN: 978-3-8439-2639-3.
- Döring, C. & Jones, P. G. (2023a). *Acta Cryst.* **E79**, 1017–1027.
- Döring, C. & Jones, P. G. (2023b). *Acta Cryst.* **E79**, 1161–1165.
- Döring, C. & Jones, P. G. (2024). *Acta Cryst.* **E80**, 157–165.
- Groom, C. R., Bruno, I. J., Lightfoot, M. P. & Ward, S. C. (2016). *Acta Cryst.* **B72**, 171–179.
- Rigaku OD (2015). (Formerly Oxford Diffraction and later Agilent Technologies.) *CrysAlis PRO*, Version 1.171.38.43 (earlier versions were also used, but are not cited separately). Rigaku Oxford Diffraction, Yarnton, England.
- Sheldrick, G. M. (2008). *Acta Cryst.* **A64**, 112–122.
- Sheldrick, G. M. (2015). *Acta Cryst.* **C71**, 3–8.